

Elastic analysis of interfacial stresses in prestressed PFGM-RC hybrid beams

Rabahi Abderezak^{*1,2}, Benferhat Rabia^{1,2a}, Tahar Hassaine Daouadji^{1,2}, Boussad Abbas³, Adim Belkacem^{2,4} and Fazilay Abbas³

¹Département de génie civil, Université Ibn Khaldoun Tiaret; BP 78 Zaaroura, Tiaret, Algérie.

²Laboratoire de Géomatique et Développement Durable, Université de Tiaret, Algérie.

³Laboratoire Grespi Campus du Moulin de la Housse, Reims Cedex 2, France

⁴Département de technologies, Centre Universitaire Tissemsilt, Algérie

(Received September 15, 2018, Revised February 16, 2019, Accepted February 24, 2019)

Abstract. In this paper, the problem of interfacial stresses in damaged reinforced concrete beams strengthened with bonded prestressed functionally graded material plate and subjected to a uniformly distributed load, arbitrarily positioned single point load, or two symmetric point loads is developed using linear elastic theory. The adopted model takes into account the adherend shear deformations by assuming a linear shear stress through the depth of the damaged RC beam. This solution is intended for application to beams made of all kinds of materials bonded with a thin FGM plate. The results show that there exists a high concentration of both shear and normal stress at the ends of the functionally graded material plate, which might result in premature failure of the strengthening scheme at these locations. Finally, numerical comparisons between the existing solutions and the present new solution enable a clear appreciation of the effects of various parameters of the beams on the distributions of the interfacial stresses.

Keywords: damaged concrete beam; prestressed plate; functionally graded material plate; interfacial stresses; strengthening

1. Introduction

The present paper is devoted to understanding the mechanism of debonding failure mode and the development of sound design rules. This brittle mode of failure is a result of the high shear and vertical normal (peeling) stress concentrations arising at the edges of the bonded composite plate. Hence, this limited area in the close vicinity of the bonded strip edge, subjected to high peeling and interfacial shear stresses, proves to be among the most critical parts of the strengthened beams. Consequently, the determination of interfacial stresses has been researched for the last decade for beams bonded with either steel or advanced composite materials. In particular, several closed-form analytical solutions have been developed Tounsi (2008), Benyoucef (2006), Tahar (2017), Chedad (2017), Khalifa (2018), Roberts (1989), Smith and teng (2001), Shen (2001), Hassaine Daouadji (2016), Yang (2007) and Bouakaz (2014). All these solutions are for linear elastic materials and

*Corresponding author, Ph.D., E-mail: rabahi.abderezak@gmail.com

^a Ph.D., E-mail: rabiebenferhat@yahoo.fr

employ the same key assumption that the adhesive is subject to normal and shear stresses that are constant across the thickness of the adhesive layer. It is this key assumption that enables relatively simple closed-form solutions to be obtained. In the existing solutions, two different approaches have been employed. Roberts (1989) and Tounsi (20018) used a staged analysis approach, Al-Emrani (2006) , Abualnour (2018), Tahar (2016), Bessegheir (2017), Hassaine Daouadji (2015), Yeghneim (2017), Adim (2018), Tlidji (2014), Benferhat (2015), Hadji (2015), Khalifa (2016), Sallai (2015), Benhenni (2018), Bensatallah (2018), Benferhat (2018), Ashraful (2018), Elghazy (2017), Gonzalez (2017), Rabahi(2016), Muhammad (2017), Meyyada (2017), Guenaneche (2014), Weu-jie (2018), Tanarlan (2017), Liang (2018), Touati (2015), Orkun (2017), Ait yahia (2015), Zidani (2015), Bousahla (2016), Bellifa (2017), El Haina (2017), Bouderbera (2016), Abdelaziz (2017), Yazid (2018), Boukhari (2016), Mensouria (2017), Youcef (2018), Bakhada (2018), Hadji (2016), Beldjillali (2016), Al Basyouni (2015) and Jian yang (2010) considered directly deformation compatibility conditions. Recently, Krour (2014), Khatir (2017), Tahar (2015), Rabia (2016), Belkacem (2016), Adim (2016), Abdelhak (2016), Lazreg (2016), Zine (2018), Attia (2018), Benchohra (2018), Hassaine Daouadji (2016) and El Mahi (2014) are developed some other methods based also on the deformation compatibility approach to predict the interfacial stresses in FRP–RC hybrid beams. Most of the research efforts have focused on strengthening of undamaged reinforced concrete beams with externally bonded sheets, whereas the interfacial stresses in damaged RC beams strengthened by externally bonded prestressed GFRP strips has not been fully studied yet. In this paper, the present study is to analyze the interfacial stresses in damaged reinforced concrete beams strengthened with bonded prestressed functionally graded material plate. The simple approximate closed – form solutions discussed in this paper provide a useful but simple tool for understanding the interfacial behaviour of an externally bonded prestressed functionally graded material plate on the damaged concrete beam with the consideration of the various parameters.

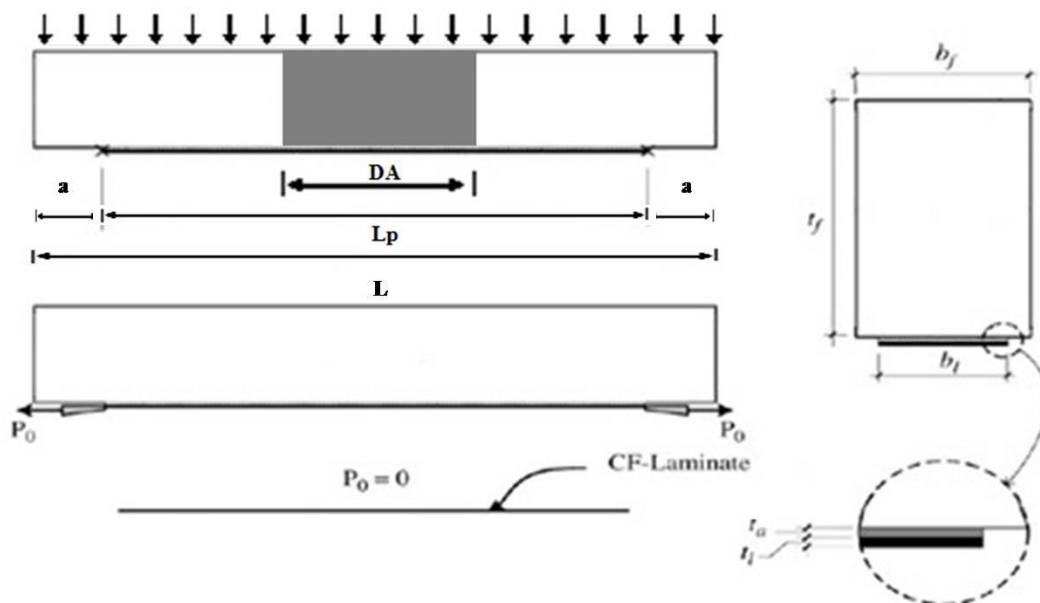


Fig. 1 Simply supported reinforced concrete beam strengthened with bonded prestressed FRP plate

2. Analytical approach

2.1 Assumptions of the solution

The following assumptions were made in the analytical study:

- All materials considered are linear elastic.
- The beam is simply supported and shallow, hence Euler Bernoulli theory.
- No slip is allowed at the interface of the bond (i.e. there is a perfect bond at the adhesive - RC beam interface and at the adhesive - plate interface).
- Bending deformations of the adhesive are neglected.
- The adhesive layer is assumed to be thin so that stresses can be considered as constant through the layers thickness.
- The bending stiffness of the RC beam to be strengthened is much greater than the stiffness of the FGM plate.

The model's Mazars (1984, 1996) is based on elasticity coupled with isotropic damage and ignores any manifestation of plasticity, as well as the closing of cracks. This concept directly describes the loss of rigidity and the softening behavior. The constraint is determined by the following relation:

$$\sigma_{ij} = (1 - \varphi) C_{ijkl} \varepsilon_{kl}, \quad 0 < \varphi < 1 \quad (1a)$$

$$\tilde{E}_{11} = E_{11}(1 - \varphi) \quad (1b)$$

$$\tilde{E}_{22} = E_{22}(1 - \varphi) \quad (1c)$$

where \tilde{E}_{11} , \tilde{E}_{22} , and E_{11} , E_{22} are the elastic constants of damaged and undamaged state, respectively, and φ is damaged variable. Hence, the material properties of the damaged plate can be represented by replacing the above elastic constants with the effective ones defined in Eq. (1b and 1c).

Basic equation of elasticity: Fig. 1 shows a schematic sketch of the steps involved in strengthening a beam with a bonded prestressed FGM plate. P_0 is the initial prestressing force in the FGM plate. P_1 is the residual prestressing force in the FGM plate upon removing the prestressing device. The loss of prestressing force in the FGM plate is thus:

$$\Delta P_1 = P_0 - P_2 \quad (2)$$

$$\text{And equilibrium requires that: } P_1 = -P_2 \quad (3)$$

Where P_s is the compression force in the beam due to prestressing.

A differential segment of a plated beam is shown in Fig. 2, where the interfacial shear and normal stresses are denoted by $\tau(x)$ and $\sigma(x)$, respectively. Fig. 2 also shows the positive sign convention for the bending moment, shear force, axial force and applied loading.

Shear stress in the adhesive layer is directly related to the difference in deformation between the FGM plate and lower flange of the steel beam:

$$\tau(x) = \frac{G_a}{t_a} [u_2(x) - u_1(x)] \quad (4)$$

Where G_a , t_a , u_1 and u_s denote the shear modulus, the thickness of the adhesive layer, the displacement of the RC beam at the bottom of lower flange, and the displacement of the externally

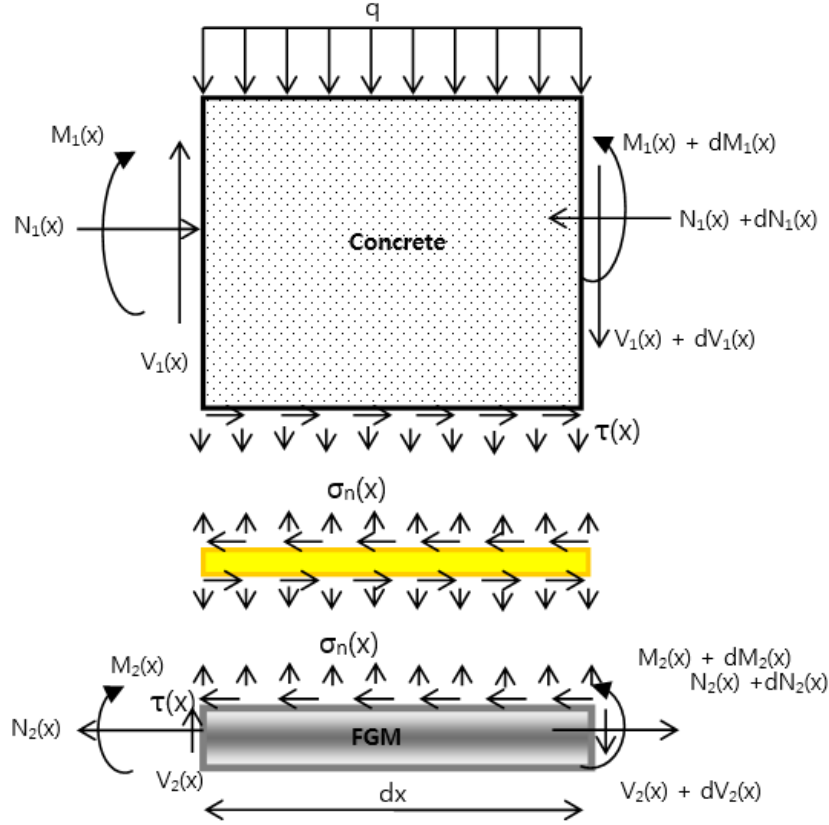


Fig. 2 Forces in infinitesimal element of a soffit-plated beam

bonded prestressed FGM plate at the boundary of the bond, respectively. Eq. (3) can be expressed in terms of the mechanical strain of the RC beam, $\varepsilon_2(x)$, and the prestressed FGM plate $\varepsilon_1(x)$ after differentiating the equation with respect to x .

$$\frac{d\tau(x)}{dx} = \frac{G_a}{t_a} [\varepsilon_2(x) - \varepsilon_1(x)] \quad (5)$$

$$\frac{du_1(x)}{dx} = \varepsilon_1(x), \quad \frac{du_2(x)}{dx} = \varepsilon_2(x) \quad (6)$$

Tensile strain at the bottom of the beam is induced by two basic stress components:

- The tensile stress induced by the bending moment $M_1(x)$ in the beam,
- The axial stress induced by the adhesive shear stress at the bond interface.

Therefore, Eq. (6) can be written as:

$$\varepsilon_1(x) = \frac{du_1(x)}{dx} = \frac{y_1}{E_1 I_1} M_1(x) + \frac{N_1}{E_1 A_1} + \frac{t_1}{4G_1} \frac{d\tau_a}{dx} \quad (7)$$

The change in axial strain in the laminate due to the deformability of the RC beam can be related to the loss in the prestressing force as follows:

$$\varepsilon_2(x) = \frac{du_2(x)}{dx} = A_{11} \frac{(N_2(x) + P_0)}{b_2} - D_{11} \frac{y_2}{b_2} M_2(x) - \frac{5t_2}{12G_2} \frac{d\tau_a}{dx} \quad (8)$$

Where u_1 and u_2 are the horizontal displacements of the concrete beam and the FGM plate respectively. M_1 and M_2 are respectively the bending moments applied to the concrete beam and the FGM plate; E_1 is Young's modulus of concrete; I_1 the moment of inertia, N_1 and N_2 are the axial forces applied to the concrete and the FGM plate respectively, t_2 and b_2 are the width and thickness of the reinforcing plate. The Young's modulus, which varies as a function of (z) , is expressed as follows:

The material properties of FGM plates are assumed to vary continuously through the thickness. The homogenization method is deployable for the computation of the Young's modulus $E(z)$ namely:

$$E(z) = E_m + (E_c - E_m) \left(\frac{z}{h} + \frac{1}{2} \right)^p \quad (9)$$

where E_m is the Young's modulus of the homogeneous plate; E_c denote Young's modulus of the bottom (as metal) and top E_c (as ceramic) surfaces of the FGM plate, respectively; E_m is Young's modulus of the homogeneous plate; and p is a parameter that indicates the material variation through the plate thickness. For the power law distribution P-FGM, the Young's modulus is given as Hassaine daouadji (2013):

Consider an imperfect FGM with a porosity volume fraction, α ($\alpha \ll 1$), distributed evenly among the metal and ceramic, the modified rule of mixture proposed by Wattanasakul pong and Ungbhakorn (2014), the Young's modulus $E(z)$ equations of the imperfect FGM beam can be expressed as:

$$E(z) = E_m + (E_c - E_m) \left(\frac{z}{h} + \frac{1}{2} \right)^p - (E_c + E_m) \frac{\alpha}{2} \quad (10)$$

E_c and E_m are the young modules of the upper and lower faces of the plate and p is the material property. Case of a sandwich: For a sandwich, plate one takes into account a heart in P-FGM.

For elastic and isotropic FGM, constitutive relations can be written as:

$$\begin{Bmatrix} \sigma_x \\ \sigma_y \\ \tau_{yz} \\ \tau_{xz} \\ \tau_{xy} \end{Bmatrix} = \begin{bmatrix} \frac{E(z)}{1-\nu^2} & \frac{\nu E(z)}{1-\nu^2} & 0 & 0 & 0 \\ \frac{\nu E(z)}{1-\nu^2} & \frac{E(z)}{1-\nu^2} & 0 & 0 & 0 \\ 0 & 0 & \frac{E(z)}{2(1+\nu)} & 0 & 0 \\ 0 & 0 & 0 & \frac{E(z)}{2(1+\nu)} & 0 \\ 0 & 0 & 0 & 0 & \frac{E(z)}{2(1+\nu)} \end{bmatrix} \begin{Bmatrix} \varepsilon_x \\ \varepsilon_y \\ \gamma_{yz} \\ \gamma_{xz} \\ \gamma_{xy} \end{Bmatrix} \quad (11)$$

where $(\sigma_x, \sigma_y, \tau_{xy}, \tau_{yz}, \tau_{xz})$ and $(\varepsilon_x, \varepsilon_y, \gamma_{xy}, \gamma_{yz}, \gamma_{xz})$ are the stress and strain components, respectively, and A_{ij}, D_{ij} are the plate stiffness, defined by:

$$A_{ij} = \int_{-\frac{h}{2}}^{\frac{h}{2}} Q_{ij} dz \quad D_{ij} = \int_{-\frac{h}{2}}^{\frac{h}{2}} Q_{ij} Z^2 dz \quad (12a)$$

\dot{A}_{11} and \dot{D}_{11} are defined as:

$$\dot{A}_{11} = \frac{A_{22}}{A_{11}A_{22} - A_{12}^2}, \quad \dot{D}_{11} = \frac{D_{22}}{D_{11}D_{22} - D_{12}^2} \quad (12b)$$

\dot{A}_{11} : Is the first term of the inverse matrix $[\dot{A}_{ij}]$ of the membrane matrix $[A_{ij}]$.

\dot{D}_{11} : Is the first term of the inverse matrix $[\dot{D}_{ij}]$ de la matrice de membrane $[D_{ij}]$.

2.2 Shear stress distribution along the FGM–concrete interface

The governing differential equation for the interfacial shear stress (Rabahi 2016) is expressed as:

$$\begin{aligned} \frac{d^2\tau(x)}{dx^2} - \frac{1}{\frac{t_a}{G_a} + \frac{t_1}{4G_1} + \frac{5t_2}{12G_2}} \left(\dot{A}_{11} + \frac{b_2}{E_1A_1} + \frac{(y_1 + y_2)(y_1 + y_2 + t_a)}{E_1I_1\dot{D}_{11} + b_2} b_2\dot{D}_{11} \right) \tau(x) \\ + \frac{1}{\frac{t_a}{G_a} + \frac{t_1}{4G_1} + \frac{5t_2}{12G_2}} \left(\frac{(y_1 + y_2)}{E_1I_1\dot{D}_{11} + b_2} \dot{D}_{11} \right) V_T(x) = 0 \end{aligned} \quad (13a)$$

For simplicity, the general solutions presented below are limited to loading which is either concentrated or uniformly distributed over part or the whole span of the beam, or both. For such loading, $d^2V_T(x)/dx^2=0$, and the general solution to Eq. (13a) is given by

$$\tau(x) = C_1 \cosh(\delta x) + C_2 \sinh(\delta x) + \frac{1}{\frac{t_a}{G_a} + \frac{t_1}{4G_1} + \frac{15t_2}{12G_2}} \left(\frac{y_1 + y_2}{E_1I_1\dot{D}_{11} + b_2} \dot{D}_{11} \right) V_T(x) \quad (13b)$$

Where:

$$\delta^2 = \frac{1}{\frac{t_a}{G_a} + \frac{t_1}{4G_1} + \frac{5t_2}{12G_2}} \left(\dot{A}_{11} + \frac{b_2}{E_1A_1} + \frac{(y_1 + y_2)(y_1 + y_2 + t_a)}{E_1I_1\dot{D}_{11} + b_2} b_2\dot{D}_{11} \right) \quad (13c)$$

And C_1 and C_2 are constant coefficients determined from the boundary conditions. In the present study, a simply supported beam was investigated which is subjected uniformly distributed load. The interfacial shear stress for this load case at any point is written as (Rabahi, 2016):

$$\begin{aligned} \tau(x) = C_1 \cosh(\delta x) + C_2 \sinh(\delta x) + \frac{1}{\frac{t_a}{G_a} + \frac{t_1}{4G_1} + \frac{15t_2}{12G_2}} \left(\frac{y_1 + y_2}{E_1I_1\dot{D}_{11} + b_2} \dot{D}_{11} \right) q \left(\frac{l}{2} - x - a \right), \\ 0 \leq x \leq L_p \end{aligned} \quad (13d)$$

Where q is the uniformly distributed load and x , a , l and L_p are defined in fig. 1. The constants of integration need to be determined by applying suitable boundary conditions:

Owing to symmetry, all displacements at the middle of the composite beam are zero.

$$u_2(x = l_p/2) = u_1(x = l_p/2) = 0 \quad (13e)$$

Which, substituted, $\tau(x = l_p/2) = 0$ and together with Eq. (13d)

$$C_1 = -C_2 \tanh\left(\delta \frac{l_p}{2}\right) \quad (13f)$$

For practical cases $\delta l_p / 2 > 10$ and as a result $\tanh\left(\frac{\delta l_p}{2}\right) \approx 1$, so the expression for C_1 can be simplified to

$$C_1 = -C_2 \quad (13g)$$

At the end of the laminate:

$$P_2(x=0) = P_1(x=0) = 0 \quad \text{and} \quad M_1(x=0) = \frac{qa}{2}(l-a) \quad (13h)$$

Inserting in Eq. (13a) gives:

$$\frac{d\tau(x=0)}{dx} = \frac{G_a}{t_a} \left[\frac{A_{11}^*}{b_2} P_0 - \frac{ha}{4E_1 I_1} q(l-a) \right] \quad (13i)$$

By substituting Eq. (13d) into Eq. (13j), C_2 can be determined as:

$$C_2 = \frac{G_a}{\delta t_a} \left[\frac{A_{11}^*}{b_2} P_0 - \frac{ha}{4E_1 I_1} q(l-a) \right] + \frac{1}{\frac{t_a}{G_a} + \frac{t_1}{4G_1} + \frac{15t_2}{12G_2}} \left(\frac{y_1 + y_2}{E_1 I_1 D_{11} + b_2} D_{11} \right) q \quad (13j)$$

Substitution of C_1 and C_2 into Eq. (13d) gives an expression for interfacial shear stress at any point:

$$\tau(x) = -C_2 e^{-\delta x} + \frac{1}{\frac{t_a}{G_a} + \frac{t_1}{4G_1} + \frac{15t_2}{12G_2}} \left(\frac{y_1 + y_2}{E_1 I_1 D_{11} + b_2} D_{11} \right) q \left(\frac{l}{2} - x - a \right) \quad (13k)$$

The distribution of the axial force in the laminate can be found by deriving Eq. (13k) once and substituting the left-hand side in Eq.(13a):

$$\delta C_2 e^{-\delta x} - \frac{1}{\frac{t_a}{G_a} + \frac{t_1}{4G_1} + \frac{15t_2}{12G_2}} \left(\frac{y_1 + y_2}{E_1 I_1 D_{11} + b_2} D_{11} \right) q = \frac{G_a}{t_a} \left(\frac{A_{11}^*}{b_2} P_0 - \frac{A_{11}^*}{b_2} P_2(x) - \frac{M_1(x) h}{I_1 E_1} + \frac{P_1(x)}{A_1 E_1} \right) \quad (13l)$$

Using the following equations ((13l) and (13m)) we obtain Eq. (13o)

$$P_2(x) = -P_1(x) \quad (13m)$$

$$M_1(x) = \frac{qa}{2}(x+a) - \frac{qa}{2}(x+a)^2 + P_2(x) \frac{h}{2} \quad (13n)$$

$$P_2(x) = \frac{b_2 G_a}{\delta^2 t_a} \frac{A_{11}^*}{b_2} P_0 (1 - e^{-\delta x}) - q \left[\frac{lh}{4E_1 I_1} (x+a) - \frac{h}{4E_1 I_1} (x+a)^2 - \frac{ha}{4E_1 I_1} (l-a) e^{-\delta x} - \frac{t_a}{G_a} \frac{1}{\frac{t_a}{G_a} + \frac{t_1}{4G_1} + \frac{15t_2}{12G_2}} \left(\frac{y_1 + y_2}{E_1 I_1 D_{11} + b_2} D_{11} \right) (1 - e^{-\delta x}) \right] \quad (13o)$$

2.3 Normal stress distribution along the FGM–concrete interface

The following governing differential equation for the interfacial normal stress (Rabahi 2016):

$$\frac{d^4 \sigma_n(x)}{dx^4} + K_n \left(D_{11} + \frac{b_2}{E_1 I_1} \right) \sigma_n(x) - K_n \left(D_{11} \frac{t_2}{2} - \frac{y_1 b_2}{E_1 I_1} \right) \frac{d\tau(x)}{dx} + \frac{q K_n}{E_1 I_1} = 0 \quad (14a)$$

The general solution to this fourth-order differential equation is

$$\sigma_n(x) = e^{-\gamma x} [C_3 \cos(\gamma x) + C_4 \sin(\gamma x)] + e^{\gamma x} [C_5 \cos(\gamma x) + C_6 \sin(\gamma x)] - \left(\frac{y_1 b_2 - \frac{D_{11} E_1 I_1 t_2}{2}}{D_{11} E_1 I_1 + b_2} \right) \frac{d\tau(x)}{dx} - \frac{1}{D_{11} E_1 I_1 + b_2} q \quad (14b)$$

For large values of x , it is assumed that the normal stress approaches zero and, as a result, $C_5 = C_6 = 0$. The general solution therefore becomes

$$\sigma_n(x) = e^{-\gamma x} [C_3 \cos(\gamma x) + C_4 \sin(\gamma x)] - \left(\frac{y_1 b_2 - \frac{D_{11} E_1 I_1 t_2}{2}}{D_{11} E_1 I_1 + b_2} \right) \frac{d\tau(x)}{dx} - \frac{1}{D_{11} E_1 I_1 + b_2} q \quad (14c)$$

Where

$$\gamma = \sqrt[4]{\frac{K_n}{4} \left(D_{11} + \frac{b_2}{E_1 I_1} \right)} \quad (14d)$$

The above expressions for the constants C_3 and C_4 has been left in terms of the bending moment $M_T(0)$ and shear force $V_T(0)$ at the end of the soffit plate. With the constants C_3 and C_4 determined, are determined by considering appropriate boundary conditions. The first boundary condition is the zero-bending moment at the ends of the soffit plate. The resulting expression yields the following relationship at the plate end, by differentiating Eq. (14c):

$$\frac{d^2 \sigma(x=0)}{dx^2} = \frac{E_a}{t_a} \left[\frac{1}{E_1 I_1} M_1(0) - \frac{D_{11}^*}{b_2} M_2(0) \right] \quad (14e)$$

However, the moment at the plate end $M_2(0)$ is zero. As a result, the above relationship can be expressed as:

$$\frac{d^2 \sigma(x=0)}{dx^2} = \frac{E_a}{t_a E_1 I_1} M_1(0) \quad (14f)$$

Boundary condition 2 concerns the shear force at the end of the soffit plate in the beam and the soffit plate. The resulting expression yields the following relationship at the plate end, by differentiating Eq. (14c):

$$\frac{d^3 \sigma(x=0)}{dx^3} = \frac{E_a}{t_a} \left[\frac{1}{E_1 I_1} V_1(0) - \frac{D_{11}^*}{b_2} V_2(0) \right] - \frac{E_a}{t_a} \left(\frac{b_2 h}{2 E_1 I_1} - \frac{t_2}{2} D_{11}^* \right) \tau(0) \quad (14g)$$

As the applied shear force at the end of the plate is zero (i.e., $V_2(0) = 0$). The second boundary condition can therefore be expressed as:

$$\frac{d^3 \sigma(x=0)}{dx^3} = \frac{E_a}{t_a E_1 I_1} V_1(0) - \frac{E_a}{t_a} \left(\frac{b_2 h}{2 E_1 I_1} - \frac{t_2}{2} D_{11}^* \right) \tau(0) \quad (14h)$$

Further differentiation of Eq. (14c) leads to the following expressions for the second and third derivatives of the interfacial normal stress at the plate end

$$\frac{d^2\sigma(x=0)}{dx^2} = -\gamma^2 C_4 - \frac{y_1 b_2 - \frac{D_{11} E_1 I_1 t_2}{2}}{D_{11} E_1 I_1 + b_2} \frac{d^3\tau(x=0)}{dx^3} - \frac{1}{D_{11} E_1 I_1 + b_2} \frac{d^2 q}{dx^2} \quad (14i)$$

$$\frac{d^3\sigma(x=0)}{dx^3} = 2\gamma^3 (C_3 + C_4) - \frac{y_1 b_2 - \frac{D_{11} E_1 I_1 t_2}{2}}{D_{11} E_1 I_1 + b_2} \frac{d^4\tau(x=0)}{dx^4} - \frac{1}{D_{11} E_1 I_1 + b_2} \frac{d^3 q}{dx^3} \quad (14k)$$

Since the loading is limited to either uniformly distributed or point loads, the second and higher order derivatives of q become zero. Substituting the boundary conditions into the above two equations then leads to the determination of C_3 and C_4 as follows:

$$C_3 = \frac{E_a}{2\gamma^3 t_a E_1 I_1} [V_1(0) + \gamma M_1(0)] - \frac{E_a}{2\gamma^3} \left(\frac{b_2 h}{2 E_1 I_1} - \frac{t_2}{2} D_{11} \right) \tau(0) + \frac{y_1 b_2 - \frac{D_{11} E_1 I_1 t_2}{2}}{2\gamma^3 (D_{11} E_1 I_1 + b_2)} \left(\frac{d^4\tau(x=0)}{dx^4} + \gamma \frac{d^3\tau(x=0)}{dx^3} \right) \quad (14l)$$

$$C_4 = -\frac{E_a}{2\gamma^2 t_a E_1 I_1} M_1(0) - \frac{y_1 b_2 - \frac{D_{11} E_1 I_1 t_2}{2}}{2\gamma^2 (D_{11} E_1 I_1 + b_2)} \frac{d^3\tau(x=0)}{dx^3} \quad (14m)$$

3. Numerical verification and discussions:

3.1 Material used

To better understand the behavior of bonded beam repairs, which will help engineers in optimizing their design parameters, the effects of several parameters were investigated. The material used for the present studies is an RC beam bonded with an FGM plate. The beams are simply supported and subjected to a different type of loading (uniformly distributed load, a single point distributed load and a Two symmetric point load). A summary of the geometric and material properties is given in table 1.

Comparison with experimental results: To validate the present method, a rectangular section is used here. One of the tested beams bonded with steel plate by Jones (1988), beams F31, is analysed here using the present improved solution. The beam is simply supported and subjected to four-point bending, each at the third point. The geometry and materials properties of the specimen are summarized in the table 1. The interfacial shear stress distributions in the beam bonded with a soffit steel plate under the applied load 180 kN, are compared between the experimental results and those obtained by the present method (FGM plate $\alpha = 0$ and $\alpha = 0,2$). As it can be seen from figure 3, the predicted theoretical results are in reasonable agreement with the experimental results.

Comparison with analytical solutions: As a part of a research project on strengthening existing RC bridges using by different class of composite materials (Carbone Fiber Reinforced Polymer, Glass Fiber Reinforced Polymer, perfect Functionally Graded Materials, imperfect Functionally Graded Materials and Sandwich Functionally Graded Materials) a demonstration study was performed on an old railway RC bridge. The aim of this study was to investigate practical

Table 1 Geometric and material properties

Component	Width (mm)	Depth (mm)	Young's modulus (MPa)	Poisson's ratio	Shear modulus (MPa)
RC beam	$b_1 = 200$	$t_1 = 300$	$E_1 = 30\,000$	0.18	-
Adhesive layer RC beam	$b_a = 200$	$t_a = 4$	$E_a = 3000$	0.35	-
GFRP plate (bonded RC beam)	$b_2 = 200$	$t_2 = 4$	$E_2 = 50\,000$	0.28	$G_{12} = 5000$
CFRP plate (bonded RC beam)	$b_2 = 200$	$t_2 = 4$	$E_2 = 140\,000$	0.28	$G_{12} = 5000$
FGM (Al_2O_3) plate (bonded RC beam)	$b_2 = 200$	$t_2 = 4$	$E_c = 380\,000$ $E_m = 70\,000$	0.3	$G_{12} = 5000$

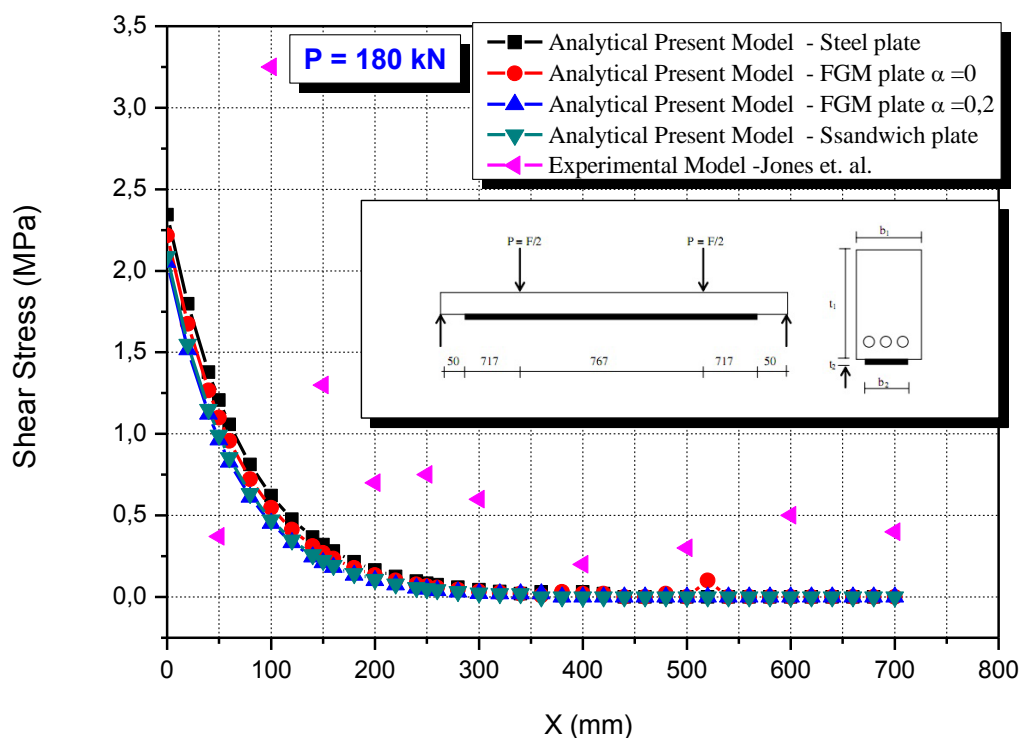


Fig. 3 Comparison of interfacial shear of the steel and FGM plated RC beam with the experimental results

difficulties that might be encountered when the strengthening technique is applied to existing structures. The beam is simply supported and subjected to a different type of loading (uniformly distributed load, a single point distributed load and a Two symmetric point load). A summary of the geometric and material properties is given in table 1. The span of The RC beam is 3000 mm and the distance from the support to the end of the plate is 300 mm. The results presented on the table 2 (2a, 2b and 2c) and figure 4 show distribution of the interfacial shear stress and the longitudinal normal stress near the plate end for the example RC beam bonded with a CFRP, GFRP, Steel, FGM and sandwich plate ($P = 0$ and $P = 80\text{kN}$) for all three types of loading (uniformly distributed load, a single point distributed load and a Two symmetric point load). It can be seen from the comparison that the stress distributions predicted by the present method are in good agreement with those obtained by using other methods.

It was recognized earlier in this study that if prestressed laminates are to be employed for strengthening this bridge, high shear and normal stresses at the end of the laminates might cause premature debonding failure of the laminates at these locations. One question was whether or not special anchorage device are needed to ensure sufficient anchorage strength. It was also recognized that there is some lack of knowledge regarding how material properties for the composite materials and the adhesives should be chosen in order to minimize the magnitude of shear and normal stresses at the ends of the laminates without reducing the efficiency of the strengthening technique.

Table 2a Comparison of interfacial shear and normal stresses (MPa): Uniformly Distributed Load

RC Beam bonded with a thin plate subjected to a uniformly distributed load													
Model	RC beam with CFRP plate		RC beam with GFRP plate		RC beam with Steel plate		RC beam with perfect FGM plate $\alpha = 0$		RC beam with imperfect FGM plate $\alpha = 0,2$		RC beam with Sandwich FGM plate		
	Shear	Normal	Shear	Normal	Shear	Normal	Shear	Normal	Shear	Normal	Shear	Normal	
Present Model	1.812	1.0893	1.093	0.832	2.126	1.176	1.994	1.113	1.826	1.060	1.861	1.113	
Rabahi 2016	1.998	1.1887	1.211	0.912	2.340	1.281	2.196	1.213	2.013	1.156	2.052	1.214	
Tounsi 2008	1.791	1.078	1.080	0.823	2.102	1.164	1.971	1.102	1.805	1.049	1.840	1.101	
RC Beam bonded with a prestressed "P = 80 kN" thin plate subjected to a uniformly distributed load													
Model	RC beam with CFRP plate		RC beam with GFRP plate		RC beam with Steel plate		RC beam with perfect FGM plate $\alpha = 0$		RC beam with imperfect FGM plate $\alpha = 0,2$		RC beam with Sandwich FGM plate		
	Shear	Normal	Shear	Normal	Shear	Normal	Shear	Normal	Shear	Normal	Shear	Normal	
Present Model	-3.037	-1.665	-7.662	-5.549	-1.754	-0.840	-2.262	-1.114	-2.975	-1.560	-2.818	-1.533	
Rabahi 2016	-3.436	-1.878	-8.598	-6.183	-2.007	-0.965	-2.572	-1.267	-3.367	-1.760	-3.192	-1.731	
Tounsi 2008	-2.991	-1.641	-7.556	-5.477	-1.725	-0.826	-2.227	-1.096	-2.931	-1.537	-2.776	-1.510	
Damaged RC Beam ($\phi=0,1$) bonded with a thin plate subjected to a uniformly distributed load													
Model	RC beam with CFRP plate		RC beam with GFRP plate		RC beam with Steel plate		RC beam with perfect FGM plate $\alpha = 0$		RC beam with imperfect FGM plate $\alpha = 0,2$		RC beam with Sandwich FGM plate		
	Shear	Normal	Shear	Normal	Shear	Normal	Shear	Normal	Shear	Normal	Shear	Normal	
Present Model	1.916	1.156	1.162	0.889	2.239	1.244	2.104	1.179	1.930	1.125	1.967	1.180	
Rabahi 2016	2.116	1.263	1.290	1.290	2.469	1.357	2.321	1.287	2.131	1.229	2.172	1.290	
Tounsi 2008	1.896	1.896	1.149	0.880	2.216	1.233	2.082	1.168	1.910	1.115	1.946	1.169	
Damaged RC Beam ($\phi=0,1$) bonded with a prestressed "P = 80 kN" thin plate subjected to a uniformly distributed load													
Model	RC beam with CFRP plate		RC beam with GFRP plate		RC beam with Steel plate		RC beam with perfect FGM plate $\alpha = 0$		RC beam with imperfect FGM plate $\alpha = 0,2$		RC beam with Sandwich FGM plate		
	Shear	Normal	Shear	Normal	Shear	Normal	Shear	Normal	Shear	Normal	Shear	Normal	
Present Model	-2.676	-1.457	-7.183	-5.209	-1.421	-0.661	-1.918	-0.928	-2.616	-1.359	-2.462	-1.327	
Rabahi 2016	-3.042	-1.653	-8.084	-5.822	-1.643	-0.770	-2.196	-1.065	-2.974	-1.543	-2.803	-1.509	
Tounsi 2008	-2.640	-1.437	-7.092	-5.147	-1.399	-0.650	-1.890	-0.914	-2.580	-1.341	-2.428	-1.309	

Table 2b Comparison of interfacial shear and normal stresses (MPa): Single Point Distributed Load

RC Beam bonded with a thin plate subjected to a Single Point Distributed Load													
Model	RC beam with CFRP plate		RC beam with GFRP plate		RC beam with Steel plate		RC beam with perfect FGM plate $\alpha = 0$		RC beam with imperfect FGM plate $\alpha = 0,2$		RC beam with Sandwich FGM plate		
	Shear	Normal	Shear	Normal	Shear	Normal	Shear	Normal	Shear	Normal	Shear	Normal	
Present Model	2.074	1.246	1.236	0.942	2.445	1.352	2.289	1.277	2.090	1.213	2.131	1.274	
Rabahi 2016	2.278	1.355	1.367	1.030	2.679	1.468	2.511	1.387	2.296	1.319	2.341	1.386	
Tounsi 2008	2.051	1.234	1.222	0.932	2.418	1.339	2.264	1.265	2.067	1.201	2.108	1.262	
RC Beam bonded with a prestressed "P = 80 kN" thin plate subjected to a Single Point Distributed Load													
Model	RC beam with CFRP plate		RC beam with GFRP plate		RC beam with Steel plate		RC beam with perfect FGM plate $\alpha = 0$		RC beam with imperfect FGM plate $\alpha = 0,2$		RC beam with Sandwich FGM plate		
	Shear	Normal	Shear	Normal	Shear	Normal	Shear	Normal	Shear	Normal	Shear	Normal	
Present Model	-2.77	-1.508	-7.51	-5.440	-1.43	-0.664	-1.96	-0.950	-2.71	-1.407	-2.54	-1.371	
Rabahi 2016	-3.15	-1.711	-8.44	-6.065	-1.66	-0.778	-2.25	-1.093	-3.08	-1.597	-2.90	-1.560	
Tounsi 2008	-2.73	-1.485	-7.41	-5.369	-1.40	-0.651	-1.93	-0.934	-2.67	-1.385	-2.50	-1.350	
Damaged RC Beam ($\phi=0,1$) bonded with a thin plate subjected to a Single Point Distributed Load													
Model	RC beam with CFRP plate		RC beam with GFRP plate		RC beam with Steel plate		RC beam with perfect FGM plate $\alpha = 0$		RC beam with imperfect FGM plate $\alpha = 0,2$		RC beam with Sandwich FGM plate		
	Shear	Normal	Shear	Normal	Shear	Normal	Shear	Normal	Shear	Normal	Shear	Normal	
Present Model	2.195	1.324	1.316	1.007	2.578	1.432	2.417	1.355	2.211	1.289	2.255	1.353	
Rabahi 2016	2.415	1.442	1.457	1.103	2.830	1.556	2.656	1.472	2.433	1.403	2.480	1.473	
Tounsi 2008	2.172	1.312	1.302	0.997	2.553	1.419	2.393	1.343	2.189	1.278	2.232	1.341	
Damaged RC Beam ($\phi=0,1$) bonded with a prestressed "P = 80 kN" thin plate subjected to a Single Point Distributed Load													
Model	RC beam with CFRP plate		RC beam with GFRP plate		RC beam with Steel plate		RC beam with perfect FGM plate $\alpha = 0$		RC beam with imperfect FGM plate $\alpha = 0,2$		RC beam with Sandwich FGM plate		
	Shear	Normal	Shear	Normal	Shear	Normal	Shear	Normal	Shear	Normal	Shear	Normal	
Present Model	-2.39	-1.288	-7.03	-5.091	-1.08	-0.473	-1.60	-0.753	-2.33	-2.334	-2.17	-1.154	
Rabahi 2016	-2.74	-1.474	-7.91	-5.695	-1.28	-0.572	-1.86	-0.880	-2.67	-1.369	-2.49	-1.326	
Tounsi 2008	-2.36	-1.270	-6.94	-5.030	-1.06	-0.463	-1.57	-0.740	-2.30	-1.178	-2.14	-1.137	

Parametric studies: Adhesive stresses without prestressing force ($P_0=0$), a comparison of the edge interfacial shear and normal stress from the different closed-form solutions reviewed earlier is undertaken in this section figure 4. In the problem, the beam is simply supported and subjected to uniformly distributed load ($q=50$ kN/ml). The results of the peak interfacial shear and normal stress are given in Tables 2a, 2b and 2c. From the presented results, it can be seen that the present solution agrees closely with the other methods. In this section, numerical results of the present solution are presented to study the effect of the prestressing force P_0 on the distribution of

interfacial stress in a steel beam strengthened with bonded prestressed FGM plate. Three value of P_0 are considered in this study ($P_0 = 0; 10; 20; 40, 80,$ and 100 kN).

Table 2c Comparison of interfacial shear and normal stresses (MPa): Two Symmetric Point Load

RC Beam bonded with a thin plate subjected to a Two Symmetric Point Load													
Model	RC beam with CFRP plate		RC beam with GFRP plate		RC beam with Steel plate		RC beam with perfect FGM plate $\alpha = 0$		RC beam with imperfect FGM plate $\alpha = 0,2$		RC beam with Sandwich FGM plate		
	Shear	Normal	Shear	Normal	Shear	Normal	Shear	Normal	Shear	Normal	Shear	Normal	
Present Model	2.718	1.590	1.733	1.290	3.126	1.680	2.956	1.601	2.737	1.543	2.783	1.619	
Rabahi 2016	3.044	1.764	1.942	1.431	3.498	1.862	3.309	1.774	3.064	1.710	3.116	1.797	
Tounsi 2008	2.682	1.570	1.709	1.274	3.084	1.659	2.917	1.581	2.700	1.524	2.746	1.599	
RC Beam bonded with a prestressed “P = 80 kN” thin plate subjected to a Two Symmetric Point Load													
Model	RC beam with CFRP plate		RC beam with GFRP plate		RC beam with Steel plate		RC beam with perfect FGM plate $\alpha = 0$		RC beam with imperfect FGM plate $\alpha = 0,2$		RC beam with Sandwich FGM plate		
	Shear	Normal	Shear	Normal	Shear	Normal	Shear	Normal	Shear	Normal	Shear	Normal	
Present Model	-2.13	-1.165	-7.022	-5.092	-0.75	-0.337	-1.30	-0.626	-2.06	-1.077	-1.89	-1.026	
Rabahi 2016	-2.38	-2.389	-7.868	-5.664	-0.84	-0.384	-1.45	-0.705	-2.31	-1.206	-2.12	-1.149	
Tounsi 2008	-2.10	-1.149	-6.927	-5.026	-0.74	-0.331	-1.28	-0.617	-2.03	-1.063	-1.87	-1.012	
Damaged RC Beam ($\phi=0,1$) bonded with a thin plate subjected to a Two Symmetric Point Load													
Model	RC beam with CFRP plate		RC beam with GFRP plate		RC beam with Steel plate		RC beam with perfect FGM plate $\alpha = 0$		RC beam with imperfect FGM plate $\alpha = 0,2$		RC beam with Sandwich FGM plate		
	Shear	Normal	Shear	Normal	Shear	Normal	Shear	Normal	Shear	Normal	Shear	Normal	
Present Model	2.861	1.678	1.836	1.371	3.279	1.768	3.105	1.687	2.880	1.629	2.928	1.709	
Rabahi 2016	3.211	1.866	2.0621	1.525	3.677	1.963	3.484	1.874	3.232	3.232	3.285	1.900	
Tounsi 2008	2.826	1.659	1.813	1.356	3.239	1.748	3.067	1.668	2.844	1.610	2.892	1.689	
Damaged RC Beam ($\phi=0,1$) bonded with a prestressed “P = 80 kN” thin plate subjected to a Two Symmetric Point Load													
Model	RC beam with CFRP plate		RC beam with GFRP plate		RC beam with Steel plate		RC beam with perfect FGM plate $\alpha = 0$		RC beam with imperfect FGM plate $\alpha = 0,2$		RC beam with Sandwich FGM plate		
	Shear	Normal	Shear	Normal	Shear	Normal	Shear	Normal	Shear	Normal	Shear	Normal	
Present Model	-1.73	-0.934	-6.510	-4.727	-0.38	-0.138	-0.91	-0.420	-1.66	-0.856	-1.50	-0.799	
Rabahi 2016	-1.94	-1.050	-7.312	-5.273	-0.43	-0.164	-1.03	-0.478	-1.87	-0.963	-1.68	-0.899	
Tounsi 2008	-1.70	-0.922	-6.429	-4.672	-0.37	-0.135	-0.90	-0.414	-1.64	-0.845	-1.48	-0.788	

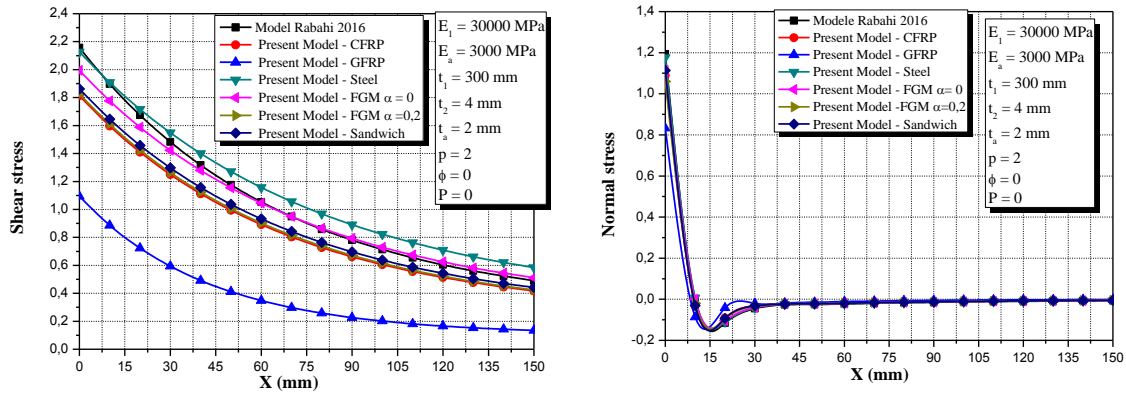


Fig. 4 Comparison of shear interfacial stress in RC beam bonded with prestressed FGM plate $P_0 = 0$

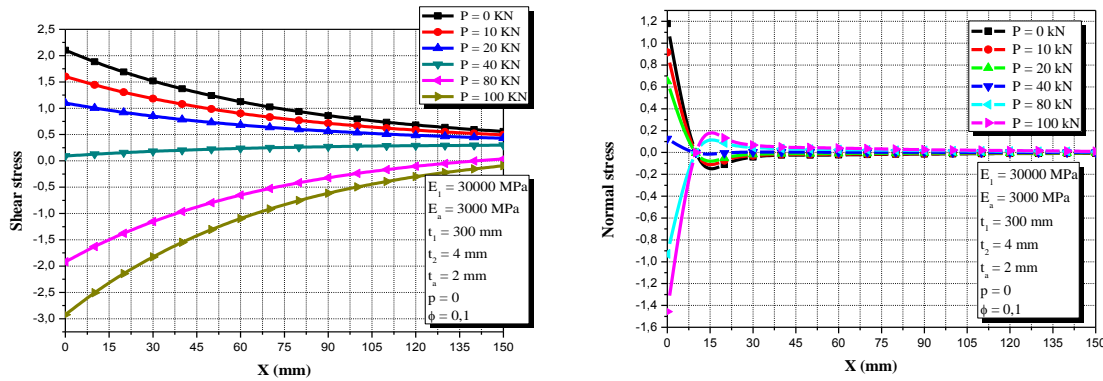


Fig. 5 Adhesive shear stress along the bond line for FGM strengthened

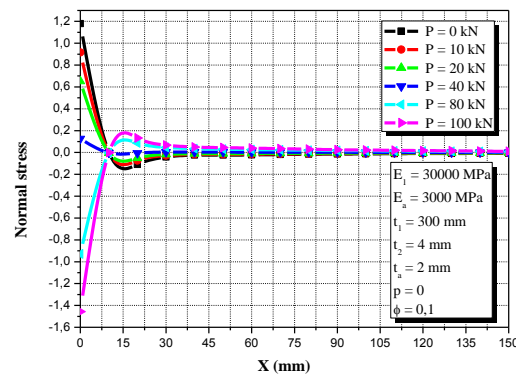


Fig. 6 Adhesive peel-off stress along the bond line for the Perfect FGM strengthened RC beam with different prestressing force P

Figs. 5 and 6 plot the interfacial shear and normal stress for the steel beam strengthened with bonded prestressed FGM plate for the mid-point load case, from these results, one can observe:

- Maximum stress occurs at the ends of adhesively bonded plates, and the normal, or peeling, stress disappears at around 20 mm from the end of the plates.
- It is seen that increasing the value of prestressing force P leads to high stress concentrations.

Effect of plate stiffness on interfacial stress: Tables 2a, 2b and 2c gives interfacial normal and shear stresses for the RC beam bonded with a CFRP, GFRP, steel and FGM plate, respectively, which demonstrates the effect of plate material properties on interfacial stresses. The length of the plate is $L_p=2400\text{mm}$, and the thickness of the plate and the adhesive layer are both 4 mm. The results show that, as the plate material becomes softer (from FGM to steel, to CFRP and then GFRP), the interfacial stresses become smaller, as expected. This is because, under the same load, the tensile force developed in the plate is smaller, which leads to reduced interfacial stresses. The position of the peak interfacial shear stress moves closer to the free edge as the plate becomes less stiff. The effect of plate stiffness on interfacial stress table 2 gives interfacial normal and shear stresses for the RC beam bonded with an FGM plate, respectively, which demonstrates the effect

of plate material properties on interfacial stresses. The results show that, as the plate material becomes softer (from FGM- Al_2O_3 and then Sandwich with homogeneous face sheet and FGM core), the interfacial stresses become smaller, as expected. This is because, under the same load, the tensile force developed in the plate is smaller, which leads to reduced interfacial stresses. The position of the peak interfacial shear stress moves closer to the free edge as the plate becomes less stiff.

Table 3 Effect of the laminate thickness of damaged RC beam bonded with a prestressed ($P = 80$ kN) thin FGM plate subjected to a uniformly distributed load

		$t_2 = 2$		$t_2 = 4$		$t_2 = 6$	
Effect of damage		Shear Stress	Normal Stress	Shear Stress	Normal Stress	Shear Stress	Normal Stress
Perfect P-FGM	$\varphi = 0$	-4,974	-4,404	-2,262	-1,114	-0,920	-0,229
	$\varphi = 0,1$	-4,568	-4,045	-1,918	-0,929	-0,607	-0,097
	$\varphi = 0,3$	-3,616	-3,198	-1,115	-0,489	0,117	0,217
Effect of damage		$t_2 = 2$		$t_2 = 4$		$t_2 = 6$	
		Shear Stress	Normal Stress	Shear Stress	Normal Stress	Shear Stress	Normal Stress
Imperfect P-FGM $\alpha = 0,1$	$\varphi = 0$	-5,3931	-2,4271	-2,593	-1,319	-1,211	-0,585
	$\varphi = 0,1$	-4,976	-2,238	-2,245	1,127	-0,891	-0,387
	$\varphi = 0,3$	-4,001	-1,794	-1,423	-0,670	-0,150	0,082
Effect of damage		$t_2 = 2$		$t_2 = 4$		$t_2 = 6$	
		Shear Stress	Normal Stress	Shear Stress	Normal Stress	Shear Stress	Normal Stress
Imperfect P-FGM $\alpha = 0,2$	$\varphi = 0$	-5,861	-5,418	-2,976	-1,560	-1,552	-0,506
	$\varphi = 0,1$	-5,432	-5,026	-2,616	-1,360	-1,224	-0,364
	$\varphi = 0,3$	-4,429	-4,099	-1,774	-0,884	-0,461	-0,027

Table 4. Effect of adhesive layer thickness of damaged RC beam bonded with a prestressed ($P = 80$ kN) thin FGM plate subjected to a uniformly distributed load

		$t_a = 1$		$t_a = 2$		$t_a = 4$	
Effect of damage		Shear Stress	Normal Stress	Shear Stress	Normal Stress	Shear Stress	Normal Stress
Perfect P-FGM	$\varphi = 0$	-2,392	-1,404	-2,262	-1,114	-2,049	-0,846
	$\varphi = 0,1$	-2,023	-1,164	-1,918	-0,929	-1,746	-0,709
	$\varphi = 0,3$	-1,171	-0,604	-1,115	-0,489	-1,020	-0,377
Effect of damage		$t_a = 1$		$t_a = 2$		$t_a = 4$	
		Shear Stress	Normal Stress	Shear Stress	Normal Stress	Shear Stress	Normal Stress
Imperfect P-FGM $\alpha = 0,1$	$\varphi = 0$	-2,742	-1,661	-2,593	-1,319	-2,357	-1,004
	$\varphi = 0,1$	-2,363	-1,411	-2,245	1,127	-2,049	-0,862
	$\varphi = 0,3$	-1,489	-0,828	-1,423	-0,670	-1,309	-0,519
Effect of damage		$t_a = 1$		$t_a = 2$		$t_a = 4$	
		Shear Stress	Normal Stress	Shear Stress	Normal Stress	Shear Stress	Normal Stress
Imperfect P-FGM $\alpha = 0,2$	$\varphi = 0$	-3,140	-1,964	-2,976	-1,560	-2,708	-1,189
	$\varphi = 0,1$	-2,750	-1,704	-2,616	-1,360	-2,393	-1,043
	$\varphi = 0,3$	-1,852	-1,094	-1,774	-0,884	-1,639	-0,686

Table 5 Effect of length of unstrengthened region “a” of damaged RC beam bonded with a prestressed (P = 80 kN) thin FGM plate subjected to a uniformly distributed load

	Effect of damage	a = 50		a = 100		a = 150		a = 200		a = 300	
		Shear Stress	Normal Stress								
Perfect P-FGM	$\varphi = 0$	-3,546	-1,832	-3,269	-1,677	-3,002	-1,527	-2,745	-1,384	-2,262	-1,114
	$\varphi = 0,1$	-3,264	-1,685	-2,974	-1,522	-2,694	-1,365	-2,424	-1,213	-1,918	-0,929
	$\varphi = 0,3$	-2,610	-1,341	-2,287	-1,157	-1,976	-0,980	-1,677	-0,810	-1,115	-0,489
Imperfect P-FGM $\alpha = 0,1$	$\varphi = 0$	-3,837	-2,026	-3,569	-1,874	-3,311	-1,727	-3,063	-1,585	-2,596	-1,320
	$\varphi = 0,1$	-3,547	-1,872	-3,266	-1,711	-2,995	-1,556	-2,735	-1,407	-2,245	-1,127
	$\varphi = 0,3$	-2,873	-1,512	-2,559	-1,330	-2,258	-1,155	-1,968	-0,987	-1,423	-0,671
Imperfect P-FGM $\alpha = 0,2$	$\varphi = 0$	-4,170	-2,254	-3,912	-2,104	-3,664	-1,960	-3,425	-1,821	-2,976	-1,560
	$\varphi = 0,1$	-3,871	-2,092	-3,600	-1,934	-3,339	-1,782	-3,088	-1,635	-2,616	-1,360
	$\varphi = 0,3$	-1,712	0,069	-2,871	-1,533	-2,580	-1,361	-2,300	-1,196	-1,774	-0,884

Effect of the laminate thickness: The thickness of the laminate plate is an important design variable in practice. Peak shear and peeling stress for various numbers of laminate layers appear in table 3. The results reveal that the number of the laminate layers significantly lowers edge peeling and shear stress. This is due to the simple fact that the initial strain will be lower for thicker laminates.

Effect of adhesive layer thickness: table 4 show the effects of the thickness of the adhesive layer on the interfacial stresses. Increasing the thickness of the adhesive layer leads to a significant reduction in the peak interfacial stresses. Thus, using thick adhesive layer, especially in the vicinity of the edge, is recommended. In addition, it can be shown that these stresses decrease during time, until they become almost constant after a very long time.

Effect of length of unstrengthened region “a”: The influence of the length of the ordinary-beam region (the region between the support and the end of the composite strip on the edge stresses) appears in table 5. It is seen that, as the plate terminates further away from the supports, the interfacial stresses increase significantly. This result reveals that in any case of strengthening, including cases where retrofitting is required in a limited zone of maximum bending moments at midspan, it is recommended to extend the strengthening strip as possible to the lines.

4. Conclusion

This paper has presented an interfacial stress analysis for damaged reinforced concrete beams strengthened with bonded prestressed functionally graded material plate under and subjected to a uniformly distributed load, arbitrarily positioned single point load, or two symmetric point loads. Such interfacial stresses provide the basis for understanding debonding failures in such RC beams

and for the development of suitable design rules. It is shown that the inhomogeneities play an important role in interfacial stresses. The obtained solution could serve as a basis for establishing simplified FGM theories or as a benchmark result to assess other approximate methodologies. The results show that the damage has a significant effect on the interfacial stresses in FGM–damaged RC beam, especially, when the length of damaged region is equal or superior to the plate length. Consequently, it is recommended to use a strengthening plate having length, superior to the damaged zone. The simplified solution to the interfacial shear stress in the prestressed FRP-plated damaged RC beams can be further exploited to develop a design method to predict the first debonding crack load. To this end, appropriate calibrations with adequate experimental results and field test data should be carried out using the reliability analysis. This is a part of our future work. We can conclude that this research is helpful for the understanding on mechanical behavior of the interface and design of the FGM–RC hybrid structures. The new solution is general in nature and may be applicable to all kinds of materials.

Acknowledgments

This research was supported by the French Ministry of Foreign Affairs and International Development (MAEDI) and Ministry of National Education, Higher Education and Research (MENESR) and by the Algerian Ministry of Higher Education and Scientific Research (MESRS) under Grant No. PHC Tassili 17MDU992. Their support is greatly appreciated.

References

- Abdelaziz, H.H., Meziane, M.A.A., Bousahla, A.A., Tounsi, A., Mahmoud, S.R. and Alwabli, A.S. (2017), “An efficient hyperbolic shear deformation theory for bending, buckling and free vibration of FGM sandwich plates with various boundary conditions”, *Steel Compos. Struct.*, **25**(6), 693-704.
- Abdelhak, Z., Hadji, L., Khelifa, Z., Hassaine daouadji, T. and El Abbes, A.B. (2016), “Analysis of buckling response of functionally graded sandwich plates using a refined shear deformation theory”, *Wind Struct.*, **22**(3), 291-305.
- Abualnour, M., Houari, M.S.A., Tounsi, A. and Mahmoud, S.R. (2018), “A novel quasi-3D trigonometric plate theory for free vibration analysis of advanced composite plates”, *Compos. Struct.*, **184**, 688-697.
- Adim, B., Hassaine Daouadji, T., Abbes, B. and Rabahi, A. (2016), “Buckling and free vibration analysis of laminated composite plates using an efficient and simple higher order shear deformation theory”, *Mech. Industry*, **17**, 512.
- Al-Basyouni, K.S., Tounsi, A. and Mahmoud, S.R. (2015), “Size dependent bending and vibration analysis of functionally graded micro beams based on modified couple stress theory and neutral surface position”, *Compos. Struct.*, **125**, 621-630.
- Al-Emrani, M. and Kliger, R. (2006), “Analysis of interfacial shear stresses in beams strengthened with bonded prestressed laminates”, *J. Compos Part B*, **37**, 265-272.
- Alam, M.A. and Al Riyami, K. (2018), “[Shear strengthening of reinforced concrete beam using natural fibre reinforced polymer laminates](#)”, *Construct. Build. Mater.*, **162**, 683-696.
- Attia, A., Bousahla, A.A., Tounsi, A., Mahmoud, S.R. and Alwabli, A.S. (2018), “A refined four variable plate theory for thermoelastic analysis of FGM plates resting on variable elastic foundations”, *Struct. Eng. Mech.*, **65**(4), 453-464.
- Bakhadda, B., Bouiadjra, M.B., Bourada, F., Bousahla, A.A., Tounsi, A. and Mahmoud, S.R. (2018), “Dynamic and bending analysis of carbon nanotube-reinforced composite plates with elastic foundation”, *Wind Struct.*, **27**(5), 311-324.

- Beldjelili, Y., Tounsi, A. and Mahmoud, S.R. (2016), "Hygro-thermo-mechanical bending of S-FGM plates resting on variable elastic foundations using a four-variable trigonometric plate theory", *Smart Struct. Syst.*, **18**(4), 755-786.
- Belkacem, A., Hassaine Daouadji, T. and Rabahi, A. (2016), "A simple higher order shear deformation theory for mechanical behavior of laminated composite plates", *IJASE*, **8**(2), 103-117.
- Belkacem, A., Hassaine Daouadji, T., Rabahi, A., Benhenni, M.A., Zidour, M. and Boussad, A. (2018), "Mechanical buckling analysis of hybrid laminated composite plates under different boundary conditions", *Struct. Eng. Mech.*, **66**(6), 761-769.
- Bellifa, H., Bakora, A., Tounsi, A., Bousahla, A.A. and Mahmoud, S.R. (2017), "An efficient and simple four variable refined plate theory for buckling analysis of functionally graded plates", *Steel Compos. Struct.*, **25**(3), 257-270.
- Benchohra, M., Driz, H., Bakora, A., Tounsi, A., El Abbes, A.B. and Mahmoud, S.R. (2018), "A new quasi-3D sinusoidal shear deformation theory for functionally graded plates", *Struct. Eng. Mech.*, **65**(1), 19-31.
- Benferhat, R., Daouadji, T.H. and Mansour, M.S. (2016), "[Free vibration analysis of FG plates resting on the elastic foundation and based on the neutral surface concept using higher order shear deformation theory](#)", *Comptes Rendus Mecanique*, **344**(9), 631-641 .
- Benferhat, R., Hassaine Daouadji, T. and Mansour, M.S. (2015), "[A Higher Order Shear Deformation Model for Bending Analysis R. of Functionally Graded Plates](#)", *Trans. Indian Inst. Met.*, **68**(1), 7-16.
- Benferhat, R., Rabahi, A., Hassaine Daouadji, T., Abbes, B., Adim, B. and Abbes, F. (2018), "[Analytical analysis of the interfacial shear stress in RC beams strengthened with prestressed exponentially-varying properties plate](#)", *Adv. Mater. Res.*, **7**(1), 29-44.
- Benhenni, M., Hassaine Daouadji, T., Abbes, B. Li, Y.M. and Abbes, F. (2018) "Analytical and numerical results for free vibration of laminated composites plates", *World Academy of Science, Engineering and Technology, J. Chem. Molecular Eng.*, **12**(6), 300-304.
- Bensattalah, T., Bouakkaz, K., Zidour, M. and Hassaine Daouadji, T. (2018), "Critical buckling loads of carbon nanotube embedded in Kerr's medium", *Adv. Nano Res.*, **6**(4), 339-356.
- Benyoucef, S., Tounsi, A., Meftah, S.A. and El Abbes, A.B. (2006), "Approximate analysis of the interfacial stress concentrations in FRP-RC hybrid beams", *Compos. Interfaces*, **13**(7), 561-571.
- Besseghier, A., Houari, M.S.A., Tounsi, A. and Mahmoud, S.R. (2017), "Free vibration analysis of embedded nanosize FG plates using a new nonlocal trigonometric shear deformation theory", *Smart Struct. Syst.*, **19**(6), 601-614.
- Bouakaz, K., Hassaine Daouadji, T., Meftah, S.A., Ameer, M. and El Abbes, A.B. (2014), "A numerical analysis of steel beams strengthened with composite materials", *Mech. Compos. Mater.*, **50**(4), 685-696.
- Bouderba, B., Houari, M.S.A., Tounsi, A. and Mahmoud, S.R. (2016), "Thermal stability of functionally graded sandwich plates using a simple shear deformation theory", *Struct. Eng. Mech.*, **58**(3), 397-422.
- Boukhari, A., Atmane, H.A., Tounsi, A., Adda, B. and Mahmoud, S.R. (2016), "An efficient shear deformation theory for wave propagation of functionally graded material plates", *Struct. Eng. Mech.*, **57**(5), 837-859.
- Bousahla, A.A., Benyoucef, S., Tounsi, A. and Mahmoud, S.R. (2016), "On thermal stability of plates with functionally graded coefficient of thermal expansion", *Struct. Eng. Mech.*, **60**(2), 313-335.
- Chaded, A., Hassaine Daouadji, T., Abderezak, R., Belkacem, A., Abbes, B., Rabia, B. and Abbes, F. (2017), "A high-order closed-form solution for interfacial stresses in externally sandwich FGM plated RC beams", *Adv. Mater. Res.*, **6**(4), 317-328.
- El-Haina, F., Bakora, A., Bousahla, A.A., Tounsi, A. and Mahmoud, S.R. (2017), "A simple analytical approach for thermal buckling of thick functionally graded sandwich plates", *Struct. Eng. Mech.*, **63**(5), 585-595.
- El Mahi, K.H.B., Belakhdar, Kh., Tounsi, A. and E.A. Adda Bedia (2014), "Effect of the tapered of the end of a FRP plate on the interfacial stresses in a strengthened beam used in civil engineering applications", *Mech. Compos. Mater.*, **50**(4), 465-474.
- Elghazy, M., El Refai, A. and Ebead, U. (2017), "[Effect of corrosion damage on the flexural performance of RC beams strengthened with FRCM composites](#)", *Compos. Struct.*, **180**(15), 994-1006.

- Ge, W.J., Ashour, A.F., Ji, X., Cai, C. and Cao, D.F. (2018), "[Flexural behavior of ECC-concrete composite beams reinforced with steel bars](#)", *Construct. Build. Mater.*, **159**, 175-188.
- Gonzalez-Libreros, J.H., Sneed, L.H. and Pellegrino, C. (2017), "[Behavior of RC beams strengthened in shear with FRP and FRCM composites](#)", *Eng. Struct.*, **150**(1), 830-842.
- Guenaneche, B., Tounsi, A. and El Abbes, A.B. (2014), "Effect of shear deformation on interfacial stress analysis in plated beams under arbitrary loading", *Adhesion Adhesives*, **48**, 1-13.
- Hadi, M.N. and Yuan, J.S. (2017) "[Experimental investigation of composite beams reinforced with GFRP I-beam and steel bars](#)", *Construct. Build. Mater.*, **144**(30), 462-474.
- Hadji, L., Hassaine Daouadji, T. and Bedia, E.A. (2016), "Dynamic behavior of FGM beam using a new first shear deformation theory", *Eartq. Struct.*, **10**(2), 451-461.
- Hadji, L., Hassaine Daouadji, T., Meziane, M.A.A., Tlidji, Y. and El Abbes, A.B. (2016), "Analysis of functionally graded beam using a new first-order shear deformation theory", *Struct. Eng. Mech.*, **57**(2), 315-325.
- Hadji, L., Khalifa, Z., Hassaine Daouadji, T., Tounsi, A. and El Abbes, A.B. (2015), "Static bending and free vibration of FGM beam using an exponential shear deformation theory", *Coupled Syst. Mech.*, **4**(1), 99-114.
- Hassaine Daouadji, T. (2017), "Analytical and numerical modeling of interfacial stresses in beams bonded with a thin plate", *Adv. Comput. Design*, **2**(1), 57-69.
- Hassaine Daouadji, T. and Belkacem, A. (2017), "Mechanical behaviour of FGM sandwich plates using a quasi-3D higher order shear and normal deformation theory", *Struct. Eng. Mech.*, **61**(1), 49-63.
- Hassaine daouadji, T. and Hadji, L. (2015) "[Analytical solution of nonlinear cylindrical bending for functionally graded plates](#)", *Geomech. Eng.* **9**(5), 631-644.
- Hassaine Daouadji, T., Abdelaziz, H.H., Tounsi, A., El Abbes, A.B. (2013), "Elasticity solution of a cantilever functionally graded beam", *Appl. Compos. Mater.*, **20**(1), 1-15
- Hassaine Daouadji, T., Benferhat, R. and Belkacem, A. (2016), "Bending analysis of an imperfect advanced composite plates resting on the elastic foundations", *Coupled Syst. Mech.*, **5**(3), 269-285.
- Hassaine Daouadji, T., Rabahi, A., Abbes, B. and Adim, B. (2016), "Theoretical and finite element studies of interfacial stresses in reinforced concrete beams strengthened by externally FRP laminates plate", *J. Adhesion Sci. Technol.*, **30**(12), 1253-1280.
- Jones, R., Swamy, R.N. and Charif, A. (1988), "Plate separation and anchorage of reinforced concrete beams strengthened by epoxy-bonded steel plates", *Struct. Eng.*, **66**(5), 85-94.
- Khalifa, Z., Hadji, L., Hassaine Daouadji, T. and Bourada, M. (2018), "[Buckling response with stretching effect of carbon nanotube-reinforced composite beams resting on elastic foundation](#)", *Struct. Eng. Mech.*, **67**(2), 125-130.
- Khalifa, Z., Hassaine Daouadji, T., Hadji, L., Tounsi, A. and El Abbes, A.B. (2016), "A new higher order shear deformation model of functionally graded beams based on neutral surface position", *Transaction. Indian Inst. Metals*, **69**(3), 683-691.
- Khetir, H., Bouiadjra, M.B., Houari, M.S.A., Tounsi, A. and Mahmoud, S.R. (2017), "A new nonlocal trigonometric shear deformation theory for thermal buckling analysis of embedded nanosize FG plates", *Struct. Eng. Mech.*, **64**(4), 391-402.
- Krouer, B., Bernard, F. and Tounsi, A. (2014), "Fibers orientation optimization for concrete beam strengthened with a CFRP bonded plate: A coupled analytical-numerical investigation", *Eng. Struct.*, **56**, 218-227.
- Liang, H., Chen, Z., Libo, Y. and Bohumil, K. (2018), "[Flexural behavior of U-shape FRP profile-RC composite beams with inner GFRP tube confinement at concrete compression zone](#)", *Compos. Struct.*, **184**, 674-687.
- Mazars, J. (1984), "Application de la mécanique de l'endommagement au comportement non linéaire et à la rupture du béton de structure", Ph.D. Dissertation, Université Paris 6, Paris.
- Mazars, J. and Pijaudier-Cabot, G. (1996), "From damage to fracture mechanics and conversely: A combined approach", *J. Solid. Struct.*, **33**(20-22), 3327-3342.
- Menasria, A., Bouhadra, A., Tounsi, A., Bousahla, A.A. and Mahmoud, S.R. (2017), "A new and simple

- HSDT for thermal stability analysis of FG sandwich plates”, *Steel Compos. Struct.*, **25**(2), 157-175.
- Meyyada, Y.A., Lesley, H.S., Omar, I.A. and ElGawady, A. (2017), “[Finite element study on the behavior of RC beams strengthened with PBO-FRCM composite under torsion](#)”, *Compos. Struct.*, **179**(1), 326-339.
- [Mori, T. and Tanaka, K. \(1973\), “Average stress in matrix and average elastic energy of materials with misfitting inclusions”](#), *Acta Metall.*, **21**, 571-574.
- Orkun Keskin, R., Arslan, G. and Sengun, K. (2017), “[Influence of CFRP on the shear strength of RC and SFRC beams](#)”, *Construct. Build. Mater.*, **153**, 16-24.
- Rabahi, A., Adim, B., Chergui, S. and Hassaine Daouadji, T. (2015), “Interfacial Stresses in FRP-Plated RC Beams: Effect of Adherend Shear Deformations”, [Multiphysics Modelling and Simulation for Systems Design and Monitoring Applied Condition Monitoring](#), **2**, 317-326 .
- Rabahi, A., Hassaine Daouadji, T., Abbas, B. and Adim, B. (2015), “Analytical and numerical solution of the interfacial stress in reinforced-concrete beams reinforced with bonded prestressed composite plate”, *J. Reinforced Plastics Compos.*, **35**(3), 258-272.
- Rabahi, A., Hassaine Daouadji, T., Benferhat, R. and Adim, B. (2018), “[Nonlinear analysis of damaged RC beams strengthened with glass fiber reinforced polymer plate under symmetric loads](#)”, *Earthq. Struct.*, **15**(2), 113-122.
- Roberts, T.M. (1989), “Approximate analysis of shear and normal stress concentrations in the adhesive layer of plated RC beams”, *Struct. Eng.*, **67**(12), 229-233.
- Sallai, B., Hadji, L., Daouadji, T.H. and Adda, B. (2015), “Analytical solution for bending analysis of functionally graded beam”, *Steel Compos. Struct.*, **19**(4), 829-841.
- Shen, H.S., Teng, J.G. and Yang, J. (2001), “Interfacial stresses in beams and slabs bonded with thin plate”, *J. Eng. Mech.*, **127**(4), 399-406.
- Smith, S.T. and Teng, J.G. (2001), “Interfacial stresses in plated beams”, *Eng. Struct.*, **23**(7), 857-871.
- Tanarlan, H.M. (2017), “[Flexural strengthening of RC beams with prefabricated ultra high performance fibre reinforced concrete laminates](#)”, *Eng. Struct.*, **151**(15), 337-348.
- Tlidji, Y., Daouadji, T.H., Hadji, L., Tounsi, A. and Bedia, E.A.A. (2014), “Elasticity solution for bending response of functionally graded sandwich plates under thermo mechanical loading” *J. Thermal Stress*, **37**, 852-869.
- Touati, M., Tounsi A. and Benguediab, M. (2015), “Effect of shear deformation on adhesive stresses in plated concrete beams: Analytical solutions”, *Comput. Concrete*, **15**(3), 141-166
- Tounsi, A., Hassaine Daouadji, T., Benyoucef, S. and Adda bedia, E.A. (2008) “Interfacial stresses in FRP-plated RC beams: Effect of adherend shear deformations”, *J. Adhesion Adhesives*, **29**(4), 343-351
- Wattanasakulpong, N. and Ungbhakorn, V. (2014), “Linear and nonlinear vibration analysis of elastically restrained ends FGM beams with porosities”, *Aerosp. Sci. Technol.*, **32**(1), 111-120.
- Yahia, S.A., Atmane, H.A., Houari, M.S.A. and Tounsi, A. (2015), “Wave propagation in functionally graded plates with porosities using various higher-order shear deformation plate theories”, *Struct. Eng. Mech.*, **53**(6), 1143-1165.
- Yang, J. and Wu, Y.F. (2007), “Interfacial stresses of FRP strengthened concrete beams: Effect of shear deformation”, *Compos. Struct.*, **80**(3), 343-351.
- Yang, J. and Ye, J. (2010) “An improved closed-form solution to interfacial stresses in plated beams using a two-stage approach”, *J. Mech. Sci.*, **52**, 13-30.
- Yang, J., Ye, J. and Niu, Z. (2007), “Interfacial shear stress in FRP-plated RC beams under symmetric loads”, *Cement Concrete Compos.*, **29**(5), 421-432.
- Yazid, M., Heireche, H., Tounsi, A., Bousahla, A.A. and Houari, M.S.A. (2018), “A novel nonlocal refined plate theory for stability response of orthotropic single-layer graphene sheet resting on elastic medium”, *Smart Struct. Syst.*, **21**(1), 15-25.
- Yeghnem, R., Guerroudj, H.Z., Amar, L.H.H., Meftah, S.A., Benyoucef, S., Tounsi, A. and Bedia, E.A.A. (2017), “Numerical modeling of the aging effects of RC shear walls strengthened by CFRP plates: A comparison of results from different code type models”, *Comput. Concrete*, **19**(5), 579-588.
- Youcef, D.O., Kaci, A., Benzair, A., Bousahla, A.A. and Tounsi, A. (2018), “Dynamic analysis of nanoscale beams including surface stress effects”, *Smart Struct. Syst.*, **21**(1), 65-74.

- Zidani, M. H. B., Belakhdar, K. and Tounsi, A. (2015), "Finite element analysis of initially damaged beams repaired with FRP plates", *Compos. Struct.*, **134**, 429-439.
- Zine, A., Tounsi, A., Draiche, K., Sekkal, M. and Mahmoud, S.R. (2018), "A novel higher-order shear deformation theory for bending and free vibration analysis of isotropic and multilayered plates and shells", *Steel Compos. Struct.*, **26**(2), 125-137.

CC